Supplementary Information

Synthesis of Composition Tunable and Highly Luminescent Cesium Lead Halide Nanowires through Anion-Exchange Reactions

Dandan Zhang[†,§,❖], Yiming Yang[†,§,❖], Yehonadav Bekenstein [†,§,||,❖], Yi Yu[†, §], Natalie A. Gibson[†,#], Andrew B. Wong[†,§], Samuel W. Eaton[†], Nikolay Kornienko[†], Qiao Kong[†], Minliang Lai[†], A. Paul Alivisatos[†,‡,§,||], Stephen R. Leone[†,#,∇], Peidong Yang[*,†,‡,§,||]

[†]Department of Chemistry, [‡]Department of Materials Science and Engineering, [∇]Department of Physics, University of California, Berkeley, CA 94720, United States

[§]Materials Sciences Division, [#]Chemical Sciences Division, Lawrence Berkeley National Laboratory, Berkeley, CA 94720, United States

[||] Kavli Energy NanoSciences Institute, Berkeley, CA 94720, United States

Experimental details:

Chemicals: Cs_2CO_3 (99.9%, Aldrich), octadecene (ODE, 90%, Aldrich), oleic acid (OA, 90%, Aldrich), $PbBr_2$ (99.999%, Alfa Aesar), PbI_2 (99%, Aldrich), oleylamine (OAm, Aldrich, 70%), octylamine (OCT, Aldrich, 99%), hexane (99.9%, Fisher Scientific), ethanol (Aldrich), molecular sieves, 4Å (Aldrich). OA, OCT and OAm were dehydrated using molecular sieves before use, other chemicals were used as received without further purification.

Preparation of Cs-oleate solution: Cs-oleate solutions were prepared via a reported approach developed by Protesescu *et al.*[1] Briefly, 0.2 g Cs_2CO_3 and 0.6 mL OA were loaded into a 3-neck flask along with 7.5 mL ODE, degassed and dried under vacuum at 120 °C (all of the temperatures mentioned in the paper is referring to the temperature of the oil bath) for 20min, and then heated under N_2 to 150 °C until all Cs_2CO_3 reacted with OA.

Preparation of oleyammonium halide (OAmX): OAmX was prepared via a reported approach developed by Nedelcu *et al.*[2]

Synthesis of $CsPbBr_3$ nanowires: 5 mL ODE and 0.2 mmol $PbBr_2$ were loaded into a 3-neck flask and degassed under vacuum for 20 min at 120 °C. 0.8 mL dried OCT and 0.8 mL dried OAm were injected at 120 °C under N_2 successively. After the injection of OCT, the solution would gradually turn a bit milky, and with the injection of OAm, the solution would turn clear. The temperature was raised to 135 °C, and the solution was stirred for 20 minutes and became opaque white. The solution was kept at 135 °C, and 0.7 mL of as-prepared Cs-oleate solution was quickly injected. After a certain duration (40 - 60 min), the reaction mixture was cooled by an ice-water bath. The NWs were isolated by centrifugation at 6000 rpm for 5 mins and washed once with hexane. The obtained precipitated NWs were re-dispersed in hexane/toluene for further use.

Surface treatment: Anhydrous toluene (5mL), $PbBr_2$ (0.188mmol, X=Cl or Br), OA (0.5mL), and OAm (0.65mL) were added to a scintillation vial all within an argon inert atmosphere glovebox. The solution was stirred at 100 °C within the glovebox until the complete dissolution of the $PbBr_2$ salt occurs, which may take several hours. The resulting concentrated stock solution is stable at room temperature, but it is stored in a glovebox to maintain the dryness of the solution over time. The cleaned nanowire solution was then mixed with the above solution and was stirred at 85 °C until the solution turned turbid, The NWs were isolated by centrifugation at 6000 rpm for 5 mins and re-dispersed in hexane/toluene for further use.

Anion-exchange reactions: The anion exchange reaction was performed under air-free conditions using standard Schlenk techniques. PbX_2 or OAmX as the anion source were mixed with ODE (5 mL) in a 3-neck flask and kept under vacuum at 100 °C for 20 min. Certain amounts of surfactants (Table S1) were injected at 100 °C under N_2 flow. After complete dissolution of the anion source, the temperature was lowered to 40 - 80 °C and $CsPbBr_3$ NWs (0.01 – 0.025 mmol) dispersed in hexane/toluene were injected to initiate the anion-exchange reaction. After reaction, the NWs were isolated by centrifugation at 6000 rpm for 5 mins and washed once with hexane. The obtained precipitated NWs were re-dispersed in hexane/toluene for further analysis.

Characterization:

Powder X-ray diffraction (XRD) patterns of the obtained products were measured on a Bruker AXS D8 Advance diffractometer with a Cu $K\alpha$ source.

The transmission electron microscopy (TEM) images, high-resolution TEM (HRTEM) images were taken with a FEI Tecnai TEM at an accelerating voltage of 200 kV.

Absorption spectra were collected using a Shimudzu UV-3010 PC UV-VIS-IR Scanning spectrophotometer equipped with a Shimadzu ISR-3100 integrating sphere.

The energy-dispersive X-ray spectroscopy (EDS) elemental mapping images were recorded using an FEI Titan microscope operated at 80 kV. This instrument was equipped with an FEI Super-X Quad windowless detector that is based on silicon drift technology. Elemental quantification data was analyzed using the Bruker Esprit EDS analysis package, which has been calibrated against mineral standards for quantitative accuracy.

Fluoresence spectra were measured on a Horiba Jobin-Yvon FluoroLog 2 spectrofluorometer.

For TRPL measurements, solutions of NWs dispersed in hexane were spin-cast onto fused silica coverslips and secured in an N_2-gas filled cell. The samples were mounted in a confocal microscope and excited in an epifluorescence scheme. The second harmonic of the output of a Coherent RegA amplifier (804 nm, 150 – 200 fs, 300 kHz) seeded by a Coherent Mira oscillator was used as the 402 nm excitation source. An MPD PDM-50 avalanche photodiode input to a Picoharp300 time-correlated single photon counting module was used to record TRPL decays with an instrument response of ~30 ps.

Transport and optoelectronic measurements were conducted on bundles of NWs under vacuum inside a probe station. Current-voltage characteristics were obtained by a Keithley 2326A dual-channel system sourcemeter. The noise level of the current is around 10 fA. The light source used for illumination in this report was a 300 W xenon lamp equipped with an air-mass 1.5 G filter (Newport). The bottom gold contacts were fabricated on a 300 nm SiO_2-coated Si chip by electron beam lithography. The surface roughness of the contacts is about 0.25 nm as measured by an atomic force microscope.

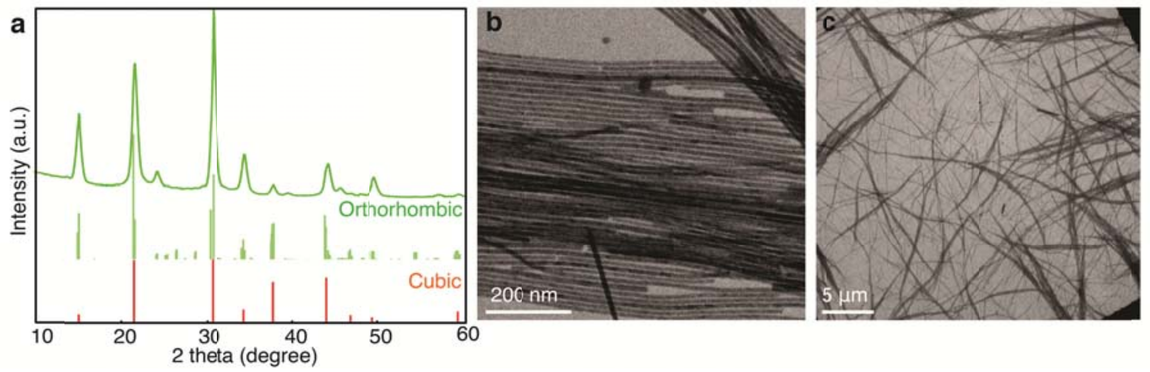

Figure S1: (a) XRD and (b, c) TEM images of the initial $CsPbBr_3$ nanowires. Standard patterns for orthorhombic and cubic $CsPbBr_3$ are provided for reference. The XRD pattern of the $CsPbBr_3$ NWs contains unique features that belong to the orthorhombic phase (peaks at ~24°, 39°, 45°); however, since the standard patterns of cubic phase mostly overlap with the orthorhombic phase, the possibility of the coexistence of some cubic phase NWs cannot be ruled out. The XRD pattern is different from our previous report,[3] because in the previous paper, the purity of the sample is not as high. The configuration of the XRD instrument has been changed to be able to afford enough signal-to-noise ratio to reveal weaker peaks in this work.

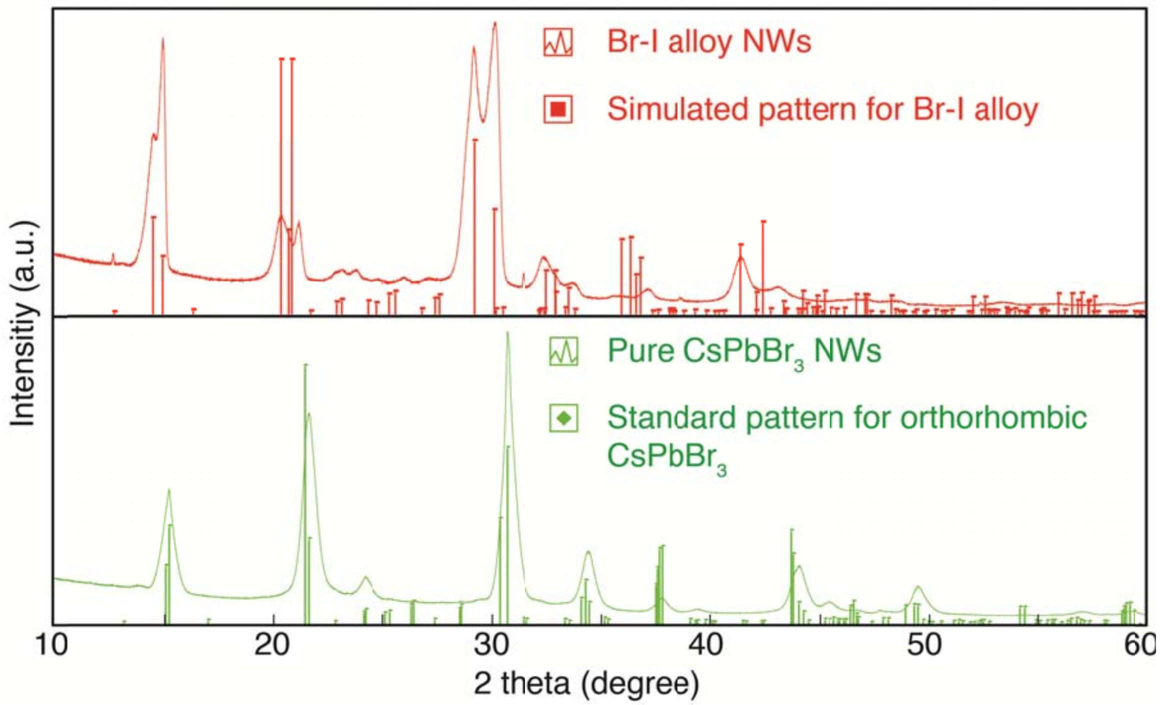

Figure S2: Experimental XRD patterns of Br-I alloy (top) and pure $CsPbBr_3$ NWs (bottom). Simulated pattern for Br-I alloy and standard pattern for orthorhombic $CsPbBr_3$ are provided for reference. The standard pattern of the Br-I alloy is simulated (using the commercially available software package 'Eva' from Bruker) by tuning the unit cell parameters of the orthorhombic $CsPbBr_3$ (By doing this, we can only fit the peak positions instead of peak intensities, since scattering power difference between Br atoms and I atoms has not been taken into consideration). The simulated pattern can fit the peak position of the Br-I experimental pattern well. The lattice parameters of the orthorhombic $CsPbBr_3$ are a = 8.207 Å, b = 8.255 Å, c = 11.759 Å. The lattice parameters of the Br-I alloy can be extracted from the simulated pattern, which are a_1 = 8.56 Å, b_1 = 8.71 Å, c_1 = 11.86 Å. The calculated lattice expansion percentage along a, b, and c direction are 4.3%, 5.5%, and 0.86%, showing an anisotropic expansion behavior.

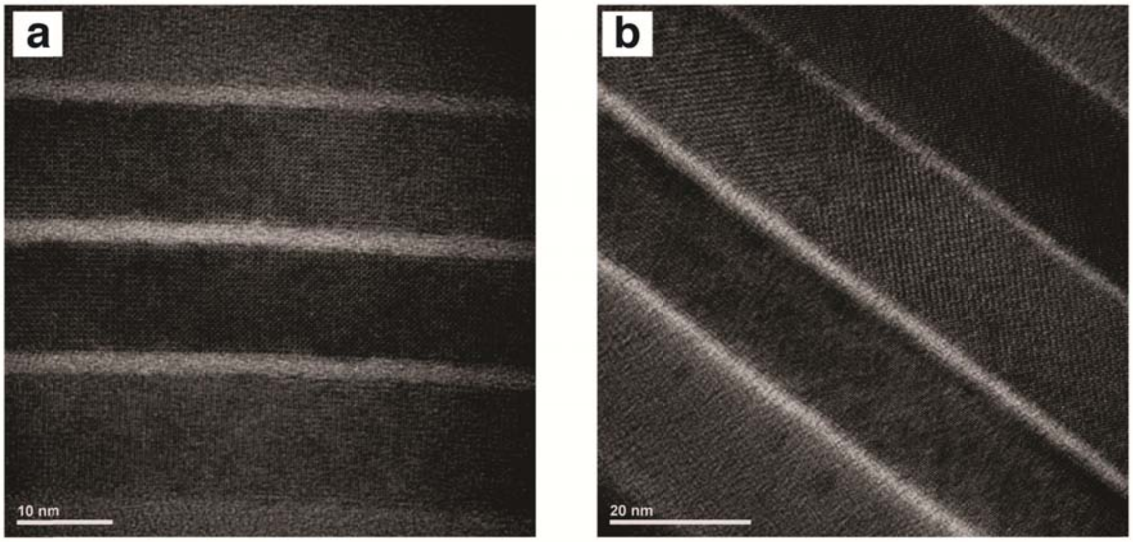

Figure S3: HR-TEM images of (a) Cl-exchanged and (b) I-exchanged NWs.

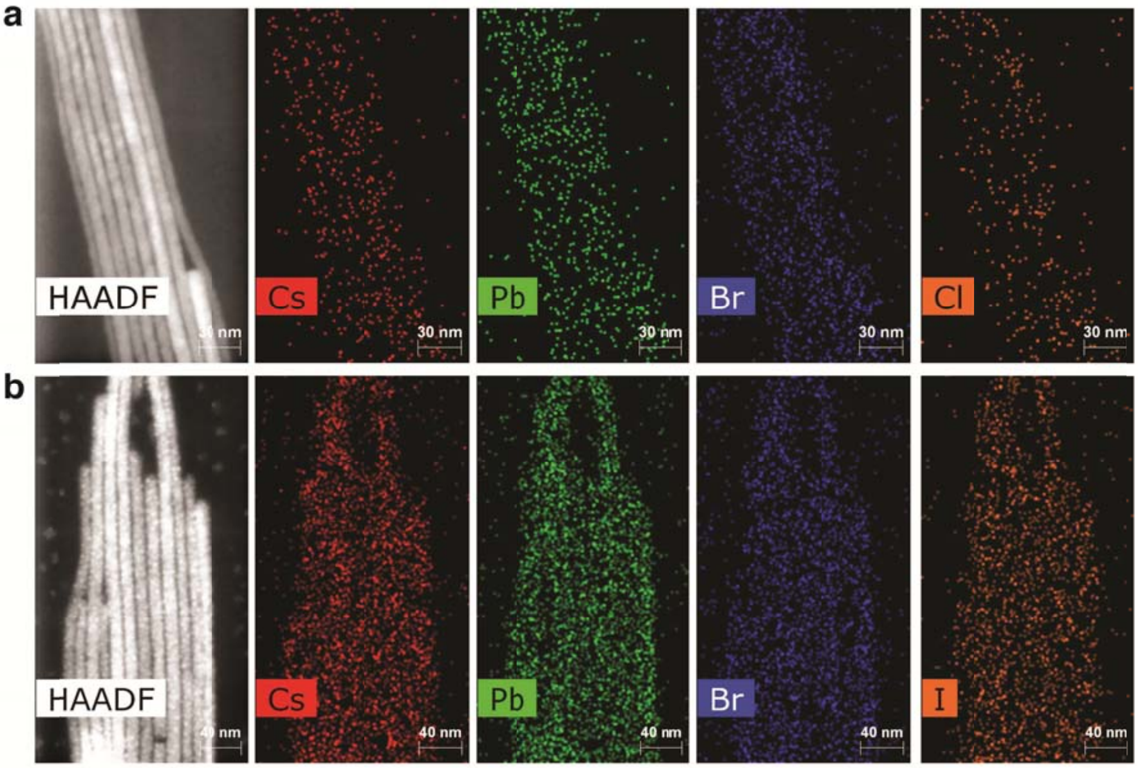

Figure S4: EDS mapping for (a) $CsPb(Br/Cl)_3$ and (b) $CsPb(Br/I)_3$ NWs after anion-exchange reactions

Table S1. Reaction parameters and the resulting PL peak positions of the products. All anion-exchange reactions were conducted in 5mL ODE at 80 °C for 10 min.

Starting NWs (mmol) estimated	Halide Precursor (mmol)	Resulting PL Peak (nm)	OA (mL)	OAm (mL)
0.01	PbI_2 – 0.824	680	0.5	0.5
0.025	PbI_2 – 0.586	678	0.3	0.3
0.025	PbI_2 – 0.347	680	0.2	0.2
0.025	PbI_2 – 0.165	674	0.2	0.2
0.025	PbI_2 – 0.087	663	0.2	0.2
0.025	PbI_2 – 0.079	649	0.2	0.2
0.025	PbI_2 – 0.043	632	0.2	0.2
0.025	PbI_2 – 0.022	586	0.2	0.2
0.025	PbI_2 – 0.011	556	0.2	0.2
0.025	OAmI – 0.891	629	0	0.2
0.025	OAmI – 0.041	551	0	0.2
0.025	OAmI – 0.012	527	0	0.2
0.025	OAmCl – 0.010	499	0	0.2
0.025	OAmCl – 0.019	481	0	0.2
0.025	OAmCl – 0.031	466	0	0.2
0.025	OAmCl – 0.260	430	0	0.2
0.025	OAmCl – 0.273	415	0	0.2
0.025	OAmCl – 0.2658	409	0	0.2

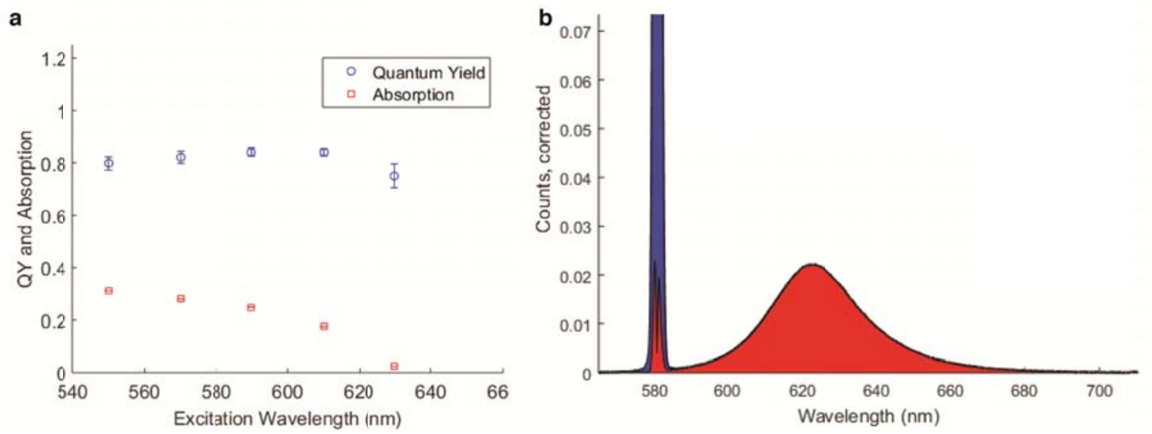

Figure S5: (a) Representative wavelength-dependent photoluminescence quantum yield and absorption plot for the best sample of I-exchanged NWs. (b) Emission spectra of the same I-exchanged sample from which the PLQY data is calculated; excitation at 580 nm is visible and highlighted in blue.

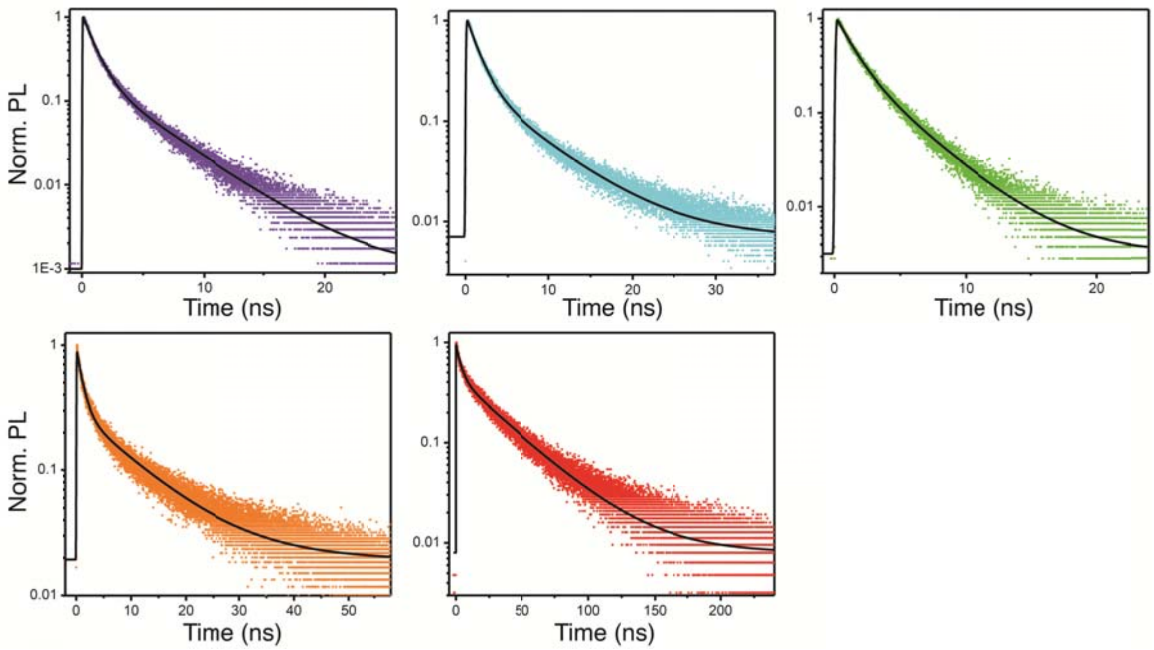

Figure S6: TRPL of $CsPbBr_3$ and alloy NWs.

Table S2. Carrier lifetimes for $CsPbBr_3$ and alloy samples.

Sample	τ_1 (ns)	τ_2 (ns)	Amplitude 1	Amplitude 2
$CsPb(Br/Cl)_3$ -1	0.94	4.46	0.84	0.16
$CsPb(Br/Cl)_3$ -2	1.48	9.07	077	0.23
$CsPbBr_3$	1.22	3.55	0.74	0.26
$CsPb(Br/I)_3$ -1	1.70	11.78	0.78	0.22
$CsPb(Br/I)_3$ -2	2.31	50.39	0.64	0.36

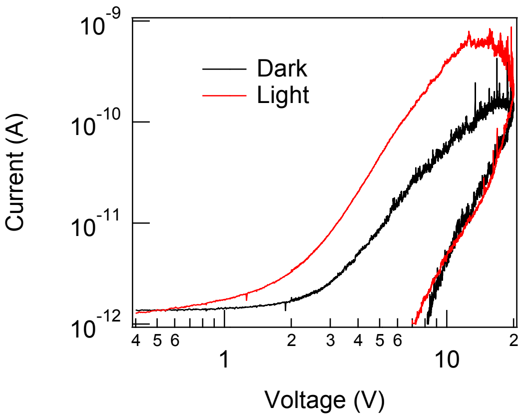

Figure S7: *I*-*V* curve of the $CsPbBr_3$ device under dark and light conditions at 300 K. The hysteresis of the *I*-*V* curves is attributed to ion migration[4]. The hysteresis is significantly reduced as the device is cooled down below 260 K.

(1) Protesescu, L.; Yakunin, S.; Bodnarchuk, M. I.; Krieg, F.; Caputo, R.; Hendon, C. H.; Yang, R. X.; Walsh, A.; Kovalenko, M. V. *Nano Lett.* 2015, 15, 3692.
(2) Nedelcu, G.; Protesescu, L.; Yakunin, S.; Bodnarchuk, M. I.; Grotevent, M. J.; Kovalenko, M. V. *Nano Lett.*2015, 15, 5635.
(3) Zhang, D.; Eaton, S. W.; Yu, Y.; Dou, L.; Yang, P. *J. Am. Chem. Soc.* 2015, 137, 9230.
(4) Yuan, Y.; Huang, J. *Acc. Chem. Res.* 2016, 49, 286.